Experimental Implementation of the Deutsch-Jozsa Algorithm for Three-Qubit Functions using Rovibrational Molecular Wave Packets Representation

Jiri Vala,[1] Zohar Amitay,[2] Bo Zhang,[2*] Stephen R. Leone,[2†] and Ronnie Kosloff[1]
[1] *Fritz Haber Research Center for Molecular Dynamics, Hebrew University, Jerusalem, 91904, Israel*
[2] *JILA, National Institute of Standards and Technology and University of Colorado, Department of Chemistry and Biochemistry, and Department of Physics, Boulder, CO 80309-0440, USA*

The Deutsch-Jozsa algorithm is experimentally demonstrated for three-qubit functions using pure coherent superpositions of Li_2 rovibrational eigenstates. The function's character, either constant or balanced, is evaluated by first imprinting the function, using a phase-shaped femtosecond pulse, on a coherent superposition of the molecular states, and then projecting the superposition onto an ionic final state, using a second femtosecond pulse at a specific time delay.

One of the benchmark quantum algorithms is the Deutsch-Jozsa algorithm [1]. Its task is to distinguish whether a binary n-qubit function $f : \{0,1\}^n \rightarrow \{0,1\}$ (n is given) is constant or balanced. The output of a constant function is identical for all possible n-qubit inputs, while the output of a balanced function is 1 for half the possible inputs and 0 for the other half. The quantum algorithm identifies the character of the function in a single call to the function, as compared to the corresponding classical algorithm that requires $2^{n-1}+1$ function evaluations to provide a solution. This improvement results from the inherent parallelism when applying the function as a unitary transformation on all the possible input elements, which are simultaneously contained within a coherent superposition.

In recent years, the Deutsch-Josza algorithm, in its revisited form [2], has been implemented experimentally mainly with NMR techniques. Using pseudopure states [3], it was demonstrated for functions having up to a four qubit input [4]. Also, an implementation of the algorithm for two-qubit functions using single photon linear optics has been published [5].

A modified version of the algorithm, which does not require a control qubit, has been proposed [6] and implemented using NMR for functions with inputs composed of up to three qubits [7]. In this version the coherent superposition representing the function domain is obtained by applying a first Hadamard rotation on the initial state $|0\rangle|0\rangle\cdots|0\rangle$ of the n-qubit system. The unitary transformation constructed for each of the various functions introduces a function dependent phase to each of the elements of the superposition. After a second n-qubit Hadamard transform is applied, the superposition either ends in the initial state if the function is constant or in any other state if it is balanced. In the present work, this modified algorithm is implemented for three-qubit functions using *pure* coherent superpositions of rovibrational molecular eigenstates (wave packets). Our main motivation behind the work is the development of a *model* system for studies of quantum information processing based on the control of *pure* coherent superpositions of multiple eigenstates, with very high degree of state-selective coherent control [8], short computation time and very low decoherence rate. In a molecule these eigenstates span several internal degrees of freedom, i.e., rotation, vibration, and electronic, a characteristic that can also be utilized to advantage.

In the current implementation of the Deutsch-Jozsa algorithm, eight rovibrational eigenstates are being used to represent the eigenstates of a system of three entangled qubits. Each three-qubit function is represented by a different unitary operation stored in an oracle, and the task is to determine whether the unitary operation applied to the molecular system corresponds to a constant or balanced function. The various unitary operations are implemented using phase-shaped broadband femtosecond pulses. The interaction of the shaped pulse with a molecule, which is initially prepared in a pure single rovibrational state, transforms the molecule into a corresponding coherent superposition of rovibrational states. Different functions result in different superpositions. The physical features of the system-field interaction allow us to apply the first Hadamard rotation and the subsequent unitary transform, representing one of the functions, in a single step. The former is associated with the amplitude transfer and the latter corresponds to the phase modification: $\hat{U}_{phs}\hat{U}_{amp}|\psi(t=0)\rangle$. The evaluation of the function's character is accomplished by probing the overall molecular superposition through its projection onto an ionic final state. This is accomplished by ionizing the molecule at a single given time delay after excitation using a second (unmodulated) femtosecond pulse. The ability to probe the overall superposition directly as a whole at one time, which originates from the quantum nature of the process, allows the readout step of the algorithm to be achieved without applying the second Hadamard rotation. The algorithm is performed on an *ensemble* of

*Permanent address: Department of Physics, Royal Institute of Technology, KTH, SE-100 44 Stockholm, Sweden
†Staff Member, Quantum Physics Devision, National Institute of Standards and Technology

molecules. Overall, only one (encoding/imprinting) unitary operation and one measurement suffice to find out the function's character.

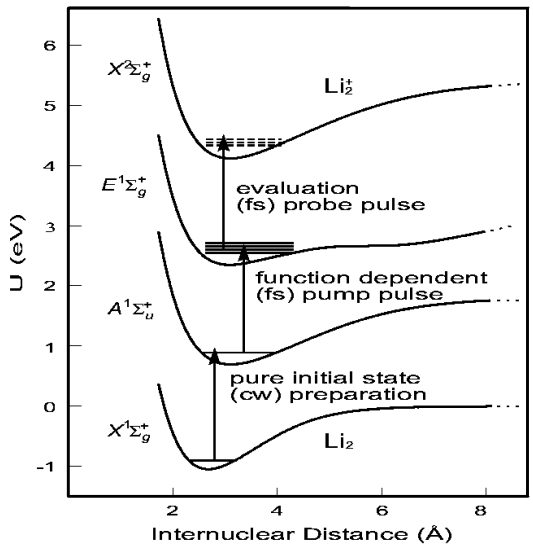

FIG. 1. Schematic picture of the excitation scheme of the experiment with the relevant potential energy curves of Li_2 and Li_2^+. The rovibrational structure of the $E^1\Sigma_g^+$ state is used for the implementation of the Deutsch-Jozsa algorithm.

The molecular excitation scheme of the experiment, with the relevant potential energy curves of Li_2 and Li_2^+, is shown in Fig. 1. The experiment [8,9] is conducted in a static cell, heated to 1023 K, that contains a lithium metal sample with Ar buffer gas. Using a cw laser, an individual transition from the thermally populated ground $X^1\Sigma_g^+$ state to the excited $A^1\Sigma_u^+$ state is selected and a single rovibrational state, $A^1\Sigma_u^+(v_A = 14, J_A = 18)$, is prepared as a pure initial state. The information that represents a function is encoded into a phase-shaped femtosecond laser pulse using a pulse shaping setup incorporating a liquid crystal spatial light modulator (128 pixels). The interaction of this shaped pulse with the Li_2 molecules, populated in the selected initial state, results in a tailored wave packet on the $E^1\Sigma_g^+$ electronic state (pump step), which for three-qubit functions is composed of $(v_E = 13 - 16, J_E = 17, 19)$ (eight states). The wave packet excitation can be described within the weak field limit [10]. Using a second (unshaped) femtosecond pulse, the wave packet is probed after a preselected delay time through the ionization of the molecule. The resulting pump-probe photoionization signal (ion and electron current) is the measured experimental quantity. It is composed of a constant signal level and a part that depends on the pump-probe delay time. The pump and probe pulses originate from a Ti:sapphire laser system with $\sim$160 fs duration, $\sim$150 cm^{-1} bandwidth, and energies of $\sim$0.5 and $\sim$1.0 μJ per pulse, respectively. The decoherence of the wave packet occurs on a time scale longer than 5 ns. It is primarily due to collisions between the Li_2 molecules and Ar and Li atoms, which result in pure dephasing and/or state-changing transitions. The decoherence time scale is at least three orders of magnitude longer than the excitation process that encodes the quantum information.

The n-qubit states are represented in a Hilbert space that includes $2^n + 1$ states: the 2^n rovibrational levels in the E-state and the single initial level in the A-state. This simplifies the implementation of the unitary operations without any principal limitation. In the present experiment, the electronic correlation between the E-state and the A-state is not probed [10], and, thus, the Hilbert space naturally reduces to the 2^n levels in the E-state. The algorithm is demonstrated here with three-qubit functions, $n = 3$, thus eight rovibrational states are employed in the E-state. Each rovibrational level, (v_E, J_E), corresponds to an eigenstate of the three-qubit product space, denoted as $|k\rangle \equiv |m\rangle|n\rangle|o\rangle$ with $m, n, o = \{0, 1\}$ where k is the decadic representation of a three-bit binary digit. Explicitly, this means that $|v_E = 13, J_E = 17\rangle \equiv |0\rangle \equiv |000\rangle$, $|v_E = 13, J_E = 19\rangle \equiv |1\rangle \equiv |001\rangle$, $|v_E = 14, J_E = 17\rangle \equiv |2\rangle \equiv |010\rangle$, $|v_E = 14, J_E = 19\rangle \equiv |3\rangle \equiv |011\rangle$, $|v_E = 15, J_E = 17\rangle \equiv |4\rangle \equiv |100\rangle$, $|v_E = 15, J_E = 19\rangle \equiv |5\rangle \equiv |101\rangle$, $|v_E = 16, J_E = 17\rangle \equiv |6\rangle \equiv |110\rangle$, and $|v_E = 16, J_E = 19\rangle \equiv |7\rangle \equiv |111\rangle$.

The unitary transformation that represents a function is generated by the Hamiltonian,

$$\hat{H} = \begin{pmatrix} \hat{H}_g & c_0^*\Omega_0^* & c_1^*\Omega_1^* & \cdots \\ c_0\Omega_0 & \hat{H}_{e0} & 0 & \\ c_1\Omega_1 & 0 & \hat{H}_{e1} & \\ \vdots & & & \ddots \end{pmatrix} . \qquad (1)$$

The symbols $\Omega_k = \mu_k\epsilon_k(t)exp(-i\omega_k t)$ $(k = 0 - 7)$ are the amplitudes acquired by the rovibrational levels on the E-state following their excitation by a transform limited (i.e., phase-unshaped) pump pulse from the initial rovibrational level on the A-state. Each amplitude Ω_k is determined by the transition dipole moment μ_k between the initial state and the excited state k, and by the spectral magnitude $\epsilon_k(t)$ of the field at the specific excitation frequency ω_k between these two states. The time-dependence of the spectral magnitude reflects the pulsed character of the field. The quantities $c_k = exp(-i\phi_k)$ include additional phase factors, ϕ_k, that are introduced to the excited rovibrational level by the phase shaping of the pump pulse. In the current description the influence of off-resonant coupling is neglected. The $\hat{H}_{ek}$ are the field-free Hamiltonians of the various excited rovibrational levels, and they are equal to the energies of the levels, i.e., $\hat{H}_{ek} = \hbar\omega_k$. Similarly, $\hat{H}_g$ corresponds to the initial level on the A-state. Under weak field conditions, the excited wave function on the electronic E potential can be formulated by first order perturbation theory [8,10]. After eliminating the A-state dynamics by

putting $H_g = 0$, the excited superposition on the E-state is given at time τ after excitation, when the pump pulse is over, as $|\psi_e(\tau)\rangle \propto \sum_{k=0}^{7} e^{-i\phi_k}\mu_k\epsilon_k e^{-i\omega_k\tau}|k\rangle$ [10]. As noted above, $k \equiv (v_E, J_E)$ while $|k\rangle$ represents the rovibrational eigenfunction of state k on the E-state. The molecule-field interaction excites each molecular level with a phase and amplitude that are controlled experimentally by shaping the excitation pulse.

Following the formulation of the modified Deutsch-Jozsa algorithm [6], the present pulse shaping is carried out to correspond to a function f such that $|\psi_e(\tau)\rangle \propto \sum_{k=0}^{7} a_k e^{-i\omega_k\tau}(-1)^{f(|k\rangle)}|k\rangle$, where a_k denotes the complex amplitude for a level k on the electronic E-state, which is independent of the specific evaluated (constant/balanced) function. Note, not all the a_k are necessarily equal. The term $(-1)^{f(|k\rangle)}$ introduces the function dependent phase factor. The 0 and 1 values of the function are encoded as a phase of 0° or 180° (i.e., a +1 or −1 factor), respectively. As a result the expansion in first order perturbation theory, $\hat{U} = \hat{1} - i\hat{H}t$, provides a model for arbitrary phase and amplitude transfer, $\hat{U} = \hat{U}_{phs}\ \hat{U}_{amp}$, from the initial A-state level onto the E-state rovibrational wave packet. It can be viewed as follows:

$$\hat{U} = \hat{U}_{phs}\ \hat{U}_{amp} = \tag{2}$$
$$\begin{pmatrix} 1 & 0 & 0 & \cdots \\ 0 & (-1)^{f(|0\rangle)} & 0 & \\ 0 & 0 & (-1)^{f(|1\rangle)} & \\ \vdots & & & \ddots \end{pmatrix} \begin{pmatrix} 1 & -a_0 & -a_1 & \cdots \\ a_0 & 1 & 0 & \\ a_1 & 0 & 1 & \\ \vdots & & & \ddots \end{pmatrix}.$$

The right term of the *r.h.s.*, $\hat{U}_{amp}$, represents the function independent part, while the left term on the *r.h.s.*, $\hat{U}_{phs}$, is the unitary operation that encodes the function values as phases. The use of perturbation theory does not represent any principle limitations, since the theory of coherent control, for a closed quantum system of a discrete spectrum, ensures that complete control can always be achieved even with strong fields [11].

Each three-qubit binary function is given as a set of eight binary (0 or 1) values, each corresponding to a possible state, $|k\rangle \equiv |m\rangle|n\rangle|o\rangle$, of a three-qubit input. There are 72 functions - 2 constant and 70 balanced. As mentioned above, a function's value of 1 is represented by a phase value of 180° and a function's value of 0 by a phase value of 0. Following the oracle operation for a given function, a set of eight phases is determined. Those phases are then encoded experimentally into the pump pulse that excites the molecular superposition. In practice, in the current experiment, we have chosen to encode these phase values into the phase-shaped pump pulse as an increment over a basic initial set of phases applied to the excited rovibrational states, $\Phi^{(0)} = \{\phi^{(0)}_{v_E,J_E}; v_E = 13-16, J_E = 17,19\}$. This $\Phi^{(0)}$ set of phases is actually part of the function independent a_k coefficients introduced above. As a result of this procedure, the two constant functions, $f_1 = \{0,0,0,0,0,0,0,0\}$ and $f_2 = \{1,1,1,1,1,1,1,1\}$, are represented by molecular superpositions having $\Phi^{(0)}$ and $\Phi^{(0)}+180°$, respectively, as their ϕ_k set of phases (see above). Since the measured pump-probe ionization signal is sensitive only to the relative phases between the various wave packet components, i.e., insensitive to a global phase of the wave packet, both constant functions correspond to the same pump-probe signal. The specific set of phases $\Phi^{(0)}$ used here is $\Phi^{(0)} = \{\phi^{(0)}_{13,17} = 298.1°, \phi^{(0)}_{13,19} = 352.0°, \phi^{(0)}_{14,17} = 215.9°, \phi^{(0)}_{14,19} = 137.9°, \phi^{(0)}_{15,17} = 169.7°, \phi^{(0)}_{15,19} = 337.6°, \phi^{(0)}_{16,17} = 192.1°, \phi^{(0)}_{16,19} = 0°\}$. These values were chosen such that the ionization of the corresponding Li_2 wave packet at 5 ps delay time after its excitation will result in a *global* maximum of the measured coherent signal [8,9]. The 5 ps time was chosen arbitrarily. The balanced functions (f_3 to f_{72}) will result in rovibrational wave packets having sets of relative phases that are different from $\Phi^{(0)}$, and, consequently, the corresponding amplitudes of the wave packet ionization signals at 5 ps delay time will be significantly lower than the global maximum signal. Hence, the identification of the function's character can be made by measuring the signal amplitude at this single predetermined delay time, after a calibration control experiment to measure the global maximum signal (i.e., for the wave packet with $\Phi^{(0)}$) is initially performed one time only.

Figure 2 displays the time-dependent part of several pump-probe ionization transients originating from various tailored wave packets; each represents a three-qubit function. Similar to the pair of constant functions, following from the insensitivity to a global phase of the wave packet, each transient actually corresponds to either of two functions, f_i and f_j, related as $f_i = \bar{f}_j$, i.e., 0 and 1 exchange in their logical representation (for example, f_3 and f_4 given below). The transient shown in all panels by the dashed lines corresponds to the constant functions (f_1 or f_2), while the transients shown in solid lines each correspond to a different pair of balanced functions. The eight balanced functions presented in the figure are $f_3 = \{0,0,0,0,1,1,1,1\}$, $f_4 = \{1,1,1,1,0,0,0,0\}$, $f_5 = \{0,1,1,1,1,0,0,0\}$, $f_6 = \{1,0,0,0,0,1,1,1\}$, $f_7 = \{1,1,0,0,0,1,1,0\}$, $f_8 = \{0,0,1,1,1,0,0,1\}$, $f_9 = \{1,1,1,0,1,0,0,0\}$, and $f_{10} = \{0,0,0,1,0,1,1,1\}$. As can be seen in the figure, measuring the coherent signal originating from the ionization of the wave packet at the single delay time of 5 ps provides the answer to whether the evaluated function is constant or balanced. The signal amplitude at 5 ps that corresponds to functions f_3 and f_4 is expected as the closest one, among all the 70 balanced functions, to the signal amplitude at 5 ps of the constant functions (f_1 and f_2). Thus, considering the experimental signal-to-noise levels with the corresponding error bars, the present probability of obtaining a cor-

rect answer about the function's character is greater than 99%. The key ingredient of the read-out procedure is a direct single access to the overall set of relative phases encoded in the rovibrational superposition.

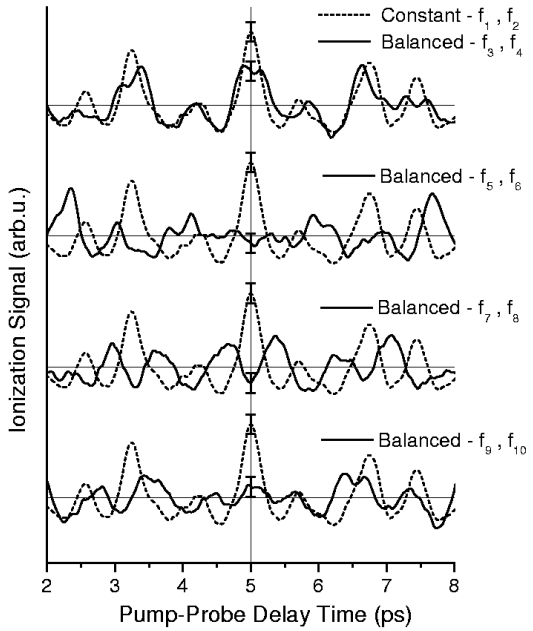

FIG. 2. Pump-probe ionization transients originating from various tailored wave packets representing various three-qubit constant or balanced functions. The f_1 and f_2 are the two constant functions, while all the other f_i are balanced. The function's character (constant/balanced) is evaluated by measuring the signal level at a single delay time of 5 ps.

The present implementation allows straightforward extension to multi-qubit binary functions beyond three qubits. This requires an increase in the number of rovibrational levels composing the excited superposition, 2^n levels for n qubits. However, from the way the functions are encoded (i.e., always half the levels are phase 0 and the other half 180°), an increase in n does not require an increase in the desired experimental signal-to-noise, i.e., there is *no* need to ionize more Li_2 molecules. Another point to mention is that the probe field can in principle be much weaker than the encoding field. This actually allows the evaluation of the function's character while keeping the encoded quantum information primarily undamaged for further use. This is important in the context of future implementation of more complicated algorithms using rovibrational molecular pure coherent superpositions.

In conclusion, we experimentally implemented the modified Deutsch-Jozsa algorithm for three-qubit functions using molecular rovibrational pure states. This task is carried out in the framework of coherent parallel computation using quantum elements [12], which we distinguish from quantum computation based on experimentally controlled entanglement. Quantum information is encoded into the relative phases of rovibrational levels that constitute the nuclear wave packet on the $E^1\Sigma_g^+$ state of the Li_2 molecule. An extension of the present scheme for multi-binary functions is possible. Measurement of the quantum state using a weak probe field allows direct and possibly non-destructive access to the relative phase information that can be preserved for further quantum operations.

This work was supported by the Israel Science Foundation, the National Science Foundation, and the Army Research Office.

[1] D. Deutsch and R. Jozsa, Proc. R. Soc. London, Ser. A **439**, 553 (1992).
[2] R. Cleve *et al.*, Proc. R. Soc. London, Ser. A **454**, 339 (1998).
[3] N. A. Gershenfeld and I. L. Chuang, Science **275**, 350 (1997).
[4] J. A. Jones and M. Mosca, J. Chem. Phys. **109**, 1648 (1998); N. Linden, H. Barjat, and R. Freeman, Chem. Phys. Lett. **296**, 61 (1998); R. Marx *et al.*, Phys. Rev. A **62**, 012310 (2000); K. Dorai, Arvind, and A. Kumar, Phys. Rev. A **61**, 042306 (2000).
[5] S. Takeuchi, Phys. Rev. A **62**, 032301 (2000).
[6] D. Collins, K. W. Kim, and W. C. Holton, Phys. Rev. A **58**, R1633 (1998).
[7] Arvind, K. Dorai, and A. Kumar, LANL, quant-ph/9909067; J. Kim *et al.*, Phys. Rev. A **62**, 022312 (2000); D. Collins *et al.*, Phys. Rev. A **62**, 022304 (2000).
[8] Z. Amitay *et al.*, Chem. Phys. **267/1**, 69 (2001).
[9] R. Uberna *et al.*, Faraday Discuss. **113**, 385 (1999).
[10] L. Pesce *et al.*, J. Chem. Phys. **114**, 1259 (2001).
[11] G. M. Huang, T. J. Tarn, and J. W. Clark, J. Math. Phys. **24**, 2608 (1983).
[12] A. N. Oraevskii, Quantum Electronics **30**, 457 (2000).